

Spatial and temporal variability of methane emissions and environmental conditions in a hyper-eutrophic fishpond

Petr Znachor^{1,2}, Jiří Nedoma¹, Vojtech Kolar^{1, 23}, Anna Matoušů¹

¹Biology Centre of Czech Academy of Sciences, v.v.i., Institute of Hydrobiology, Na Sádkách 7, České Budějovice, 37005, Czech Republic

²Faculty of Science, University of South Bohemia, Branišovská 1760, České Budějovice, 37005, Czech Republic

~~³Biology Centre of Czech Academy of Sciences, Institute of Entomology, Branišovská 31, České Budějovice, 37005, Czech Republic~~

Correspondence to: Anna Matoušů (anna.matousu@gmail.com)

Abstract. Estimations of methane (CH₄) emissions are often based on point measurements using either flux chambers or a transfer coefficient method which may lead to strong underestimation of the total CH₄ fluxes. In order to demonstrate more precise measurements of the CH₄ fluxes from an aquaculture pond, using higher resolution sampling approach we examined the spatiotemporal variability of CH₄ concentration in the water, related fluxes (diffusive and ebullitive) and relevant environmental conditions (temperature, oxygen, chlorophyll-a) during three diurnal campaigns in a hyper-eutrophic fishpond. Our data show remarkable variance spanning several orders of magnitude while diffusive fluxes accounted for only a minor fraction of total CH₄ fluxes (4.1–18.5 %). Linear mixed-effects models identified water depth as the only significant predictor of CH₄ fluxes. Our findings necessitate complex sampling strategies involving temporal and spatial variability for reliable estimates of the role of fishponds in a global methane budget.

Keywords: aquaculture, emissions, fishpond, freshwater, heterogeneity, methane

25 **1 Introduction**

26 Freshwater aquaculture ponds (fishponds) represent man-made counterparts to natural shallow lakes (Scheffer,
27 2004) which are mainly used for fish production (mostly of common carp, *Cyprinus carpio* L.) and water retention
28 in the landscape. Fishponds serve also as secondary biotope for various organisms (Kolar et al., 2021), supporting
29 noteworthy animal and plant diversity (Pokorný and Hauser, 2002). However, most fishponds suffer from high
30 fish stock densities, excessive carbon and nutrient loading from supplemental fish feeding, sewage pollution, and
31 fertiliser runoffs from agricultural catchments or nutrient mobilisation from the anoxic sediment layers (Pechar,
32 2000). As a result, the trophic structure of plankton communities has shifted towards a reduction of large
33 zooplankton and massive development of phytoplankton, especially cyanobacterial blooms (Potužák et al., 2007),
34 limiting light penetration in the water column. Rapid changes in the intensity of biological processes such as
35 photosynthesis and respiration often result in pronounced daily or seasonal fluctuations in dissolved oxygen (Baxa
36 et al., 2021), signalling decreasing ecosystem stability. The extent of anoxia, accumulation of organic biomass,
37 and rapid heating of the shallow water during summer result in enhanced production of greenhouse gases (Grasset
38 et al., 2018, Zhang et al., 2021; Bartosiewicz et al., 2021).

39 Most concerning are CH₄ emissions as freshwater aquaculture systems release more than 6 Tg CH₄ yr⁻¹ (Yuan et
40 al., 2019). Methane can be emitted via several pathways: simple molecular diffusion, ebullition (in the form of
41 bubbles released from oversaturated sediments), plant-mediated flux (Bastviken et al., 2004), but also through so
42 far neglected pathways including aeration, emissions from dry/drying sediments, or dredged organic material
43 (Kosten et al., 2020). Among all, ebullition is considered the dominant pathway (van Bergen et al., 2019; Kosten
44 et al., 2020), which can contribute 50-96 % (Casper et al., 2000; Xiao et al., 2017; van Bergen et al., 2019; Yang
45 et al., 2020; Zhao et al., 2021) to the total CH₄ flux. Along with the second important pathway – molecular
46 diffusion, both exhibit high spatiotemporal variability due to various physical and biological factors acting on very
47 short time scales, for instance, temperature (van Bergen et al., 2019), ~~eutrophication-nutrient loading~~ (Zhang et al.,
48 2021), ~~water depth (DeSontro et al., 2016)~~, CH₄ production rates (Zhou et al., 2019), CH₄ oxidation rates
49 (Sanseverino et al., 2012), dissolved oxygen concentration (Xiao et al., 2017), management regime (Yang et al.,
50 2019), or the quality of organic matter in the sediment (Schmiedeskamp et al., 2021). Recently, the direct
51 involvement of phytoplankton in CH₄ production and emissions has been emphasised (Yan et al., 2019; Bižić et
52 al., 2020; Bartosiewicz et al., 2021). The complex interactions between physical and biological factors lead to a
53 dynamic and ever-changing environment, characterised by high spatial and temporal variability of methane fluxes
54 in ponds.

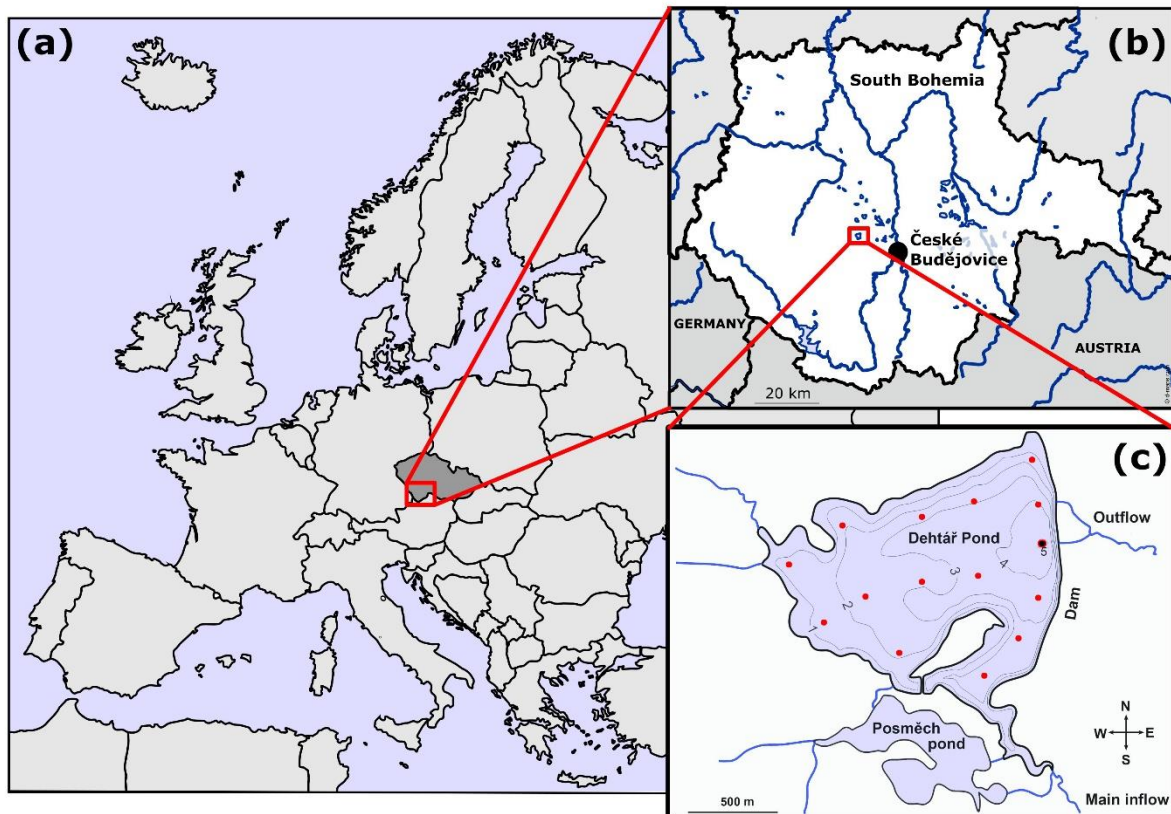
55 Although fishponds are recognised as powerful model systems for studies in ecology and evolutionary or
56 conservation biology (De Meester et al., 2005; Céréghino et al., 2008), the extent of environmental heterogeneity
57 in fishponds and shallow inland small waterbodies remains poorly understood (Ortiz and Wilkinson, 2021),
58 largely because the driving factors are either system-specific or highly variable on short time scales (Laas et al.,
59 2012). Most of current information on lentic ecosystem structure and function comes from single-site sampling,
60 in which measurements are taken over time at the deepest point in the lake, which does not sufficiently account
61 for within-lake spatial variation (Stanley et al., 2019). The motivation for our study was the growing concern about
62 the role of fishponds as important sources of CH₄ fluxes to the atmosphere (Wik et al., 2016). Unfortunately, the
63 majority of global CH₄ flux estimates rely on upscaling methods (DelSontro et al., 2018a) based on a limited
64 number of measurements that do not account for diurnal and seasonal variability or ecosystem spatial
65 heterogeneity. Yang et al. (2019) indicates that a larger number of spatial replicates over a number of months is
66 mandatory to improve the accuracy of whole-pond CH₄ flux estimates. The published research from other
67 aquaculture studies have been performed mainly in tropical and subtropical zones in fish or crab aquacultures (e.g.,
68 Hu et al., 2016; Ma et al., 2018; Yang et al., 2019, 2020; Yuan et al., 2019, 2021). To better understand the spatial
69 dynamics of CH₄ fluxes and environmental heterogeneity in temperate freshwater shallow lake, we conducted a
70 spatial sampling of the hyper-eutrophic Dehtář fishpond (Czech Republic, Europe). Since the seasonal CH₄
71 production is strongly affected by temperature, we focused on warm summer months where the total CH₄ fluxes
72 were expected to be the highest (Jansen et al., 2019). The objectives of our study were (i) to determine the spatial
73 heterogeneity of CH₄ diffusive and total fluxes and fundamental limnological variables (oxygen, temperature,
74 chlorophyll-a) and [their](#) change daily and monthly in the hyper-eutrophic pond, and (ii) to identify the factors that
75 influence CH₄ fluxes to improve our understanding of the importance of spatiotemporal variability for global
76 estimates of CH₄ efflux to the atmosphere.

77 **2 Material and Methods**

78 **2.1 Study site description**

79 The Dehtář fishpond (49° N, 14° E) is a shallow man-made lake (average and maximum depth: 2.4 and 6 m)
80 constructed in 1479 and used for polycultural, semi-intensive production of common carp (Potužák et al., 2016).
81 It lies in a flat agricultural landscape at 406.4 m above sea level in the upper Vltava River basin in South Bohemia
82 (Czech Republic) which is characteristic with its network of fishponds (Fig. 1b). Due to the orography of the

83 landscape, the Dehtář fishpond, surrounded by narrow belts of littoral vegetation and adjacent to grassland and
84 arable land, is exposed to wind, mainly from the northwest (for aerial photograph, see Suppl. Fig 1). The catchment
85 area is 91.4 km². The main inflow is the Dehtářský stream in the south, while several smaller tributaries flow in
86 from the west (Fig. 1c). The fishpond has a dam 234 m long and 10 m high, with two outlets and a safety spillway.
87 Covering 2.28 km², the Dehtář fishpond is among the ten largest fishponds in the Czech Republic, holding a
88 volume of $4.71 \times 10^3 \text{ m}^3$ and having a water residence time of 146-445 days (Potužák et al., 2016).



89
90 **Figure 1.** Location (a, b; copyright www.d-maps.com; https://d-maps.com/carte.php?num_car=2232&lang=en and https://d-maps.com/carte.php?num_car=265046&lang=en; modified) and bathymetric map (c; credit Jiří Jarošík) of the sampled Dehtář
91 fishpond: Blue lines indicate hydrological connections; red dots representing the sampling points. Highlighted sampling point
92 at the dam depicts the deepest site where vertical profiles were measured. Numbers indicate isobath depth.
93

94

95 2.2 Sampling design and measurement

96 To measure spatial heterogeneity and temporal changes in limnological parameters and methane fluxes, we
97 conducted three 36-hour surveys in summer 2019 (July 2-3, August 13-14, September 19-20). In the morning
98 (between 5-6 a.m.), we first measured surface values and vertical profiles of temperature, oxygen, and chlorophyll-
99 *a* concentration at the deepest point (see below for details). We subsequently installed 15 floating polyethylene
100 chambers (as shown in Fig. 1c), serving as fixed sampling sites and at the same time for accumulation of CH₄
101 fluxes (see further), starting in the western part of the fishpond. During installation (and further during each

102 sampling), temperature, pH, and oxygen concentration were measured at 0.3 m depth using the WTW 330i pH
103 meter and Oximeter (WTW, Weilheim, Germany). Vertical chlorophyll-*a* profiles were measured at each sampling
104 site using a submersible fluorescence probe (FluoroProbe, bbe_Moldaenke, Kiehl, Germany). From each site, the
105 average chlorophyll-*a* concentration in the surface layer (0-1 m depth) was used to assess the phytoplankton spatial
106 heterogeneity.

107 To minimise the chance that the differences observed among sites were due to time of day, we conducted repeated
108 measurements at the deepest point at the end of each sampling. This was relevant mainly to the initial measurement,
109 when the installation of all floating chambers took a total of 3 hours and 50 minutes. All other measurements, i.e.
110 the interval between the first and last sampling point, required approximately two hours each. If there was a change,
111 all values were corrected for the sampling time by linear interpolation:

$$112 \quad P_{corr} = P_t + (P_{end} - P_0) \times \frac{(t-t_0)}{(t_{end}-t_0)} \quad (1)$$

113 where P_{corr} is the corrected value of a parameter, P_t is its value measured at the time t , P_0 and P_{end} are parameter
114 values measured at the deepest point at the start (time t_0) and at the end (t_{end}) of the sampling. In the evening and
115 morning of the second day (roughly at 12 h intervals), we performed additional measurements of spatial
116 heterogeneity, allowing us to assess diurnal and nocturnal changes. In addition, samples for measuring CH_4
117 concentration in the surface water were collected at each site and analysed as described below. To assess diurnal
118 variations in thermal structure and oxygen concentration in the water column, we made vertical profile
119 measurements at the deepest point ([Fig. 1c](#)) at 3-6 h intervals using the YSI EXO 2 multiparametric probe (YSI
120 Inc., Yellow Springs, USA).

121 **2.3 Methane measurements**

122 Water samples for determining CH_4 concentration in the surface water were collected at all 15 sampling sites in
123 triplicates into 20 ml glass bottles. The bottles were capped bubble-free under water with black butyl rubber
124 stoppers (Ochs, Germany) and sealed with aluminium crimps. Immediately after sampling, the water samples were
125 preserved by injecting 100 μ l of concentrated sulfuric acid to stop the microbial activity (Bussmann et al., 2015).
126 The samples were processed within one week in the laboratory using a headspace technique according to
127 McAuliffe (1971). Methane concentration in the headspace was measured using an HP 5890 Series II gas
128 chromatograph (Agilent Technologies, USA) and calculated with the solubility coefficient given by Yamamoto et
129 al. (1976).

130 Methane diffusive fluxes (F) were then calculated for each sampling site indirectly using the 2-layer model with
131 the equation:

132 $F = k(C_{sur} - C_{eq})$ (2)

133 where C_{sur} is the CH₄ concentration in surface water in $\mu\text{mol L}^{-1}$, C_{eq} is the CH₄ concentration in surface water in
 134 equilibrium with the atmosphere in $\mu\text{mol L}^{-1}$, and k is the CH₄ exchange constant (cm h^{-1}). [The atmospheric partial
 135 pressure of CH₄ was set to 1.8 ppm. To compute \$k\$ values we first derived \$k_{600}\$ estimates using a wind speed-based
 136 relationship according to Crusius and Wanninkhof \(2003\):](#)

137 $k_{600} = 1.68 + (0.228 \times U_{10}^{2.3})$ (3)

138 [where \$U_{10}\$ represents the wind speed at 10 m height \(in \$\text{m.s}^{-1}\$; obtained from the nearby gauging station\)
 139 approximated by \$U_{10} = 1.22U\$, where \$U\$ is the wind speed at 1.5 m height. We then converted \$k_{600}\$ to \$k\$ using the
 140 eq. 4 according to Crusius and Wanninkhof \(2003\):](#)

141 $k = k_{600} \left(\frac{Sc}{600}\right)^n$ (4)

142 where k_{600} is the gas transfer velocity [for a Schmidt number \(\$Sc\$ \) of 600; \$n\$ is a wind speed-dependent conversion
 143 factor, for which we used \$-2/3\$ for \$U_{10} < 3.7 \text{ m s}^{-1}\$ \(Jähne et al., 1987\). The Schmidt number for CH₄ was calculated
 144 according to Wanninkhof \(2014\):](#)

145 $Sc = 1909.4 - 120.78t + 4.1555t^2 - 0.080578t^3 + 0.000658t^4$ (5)

146 where t ($^{\circ}\text{C}$) is the water temperature at the time of CH₄ extraction. The parameter C_{eq} in Eq. (1) was determined
 147 from the equation:

148 $C_{eq} = \beta \times pCH_4$ (6)

149 where β is the solubility coefficient of CH₄ as a function of temperature according to Wiesenburg and Guinasso
 150 (1979), and pCH_4 is the partial pressure of CH₄ in the atmosphere.

151 To estimate total CH₄ fluxes from the water column to the atmosphere (i.e., diffusive and ebullitive fluxes), we
 152 measured CH₄ accumulation in open-bottom floating polyethylene chambers (volume 3.1 L; area 0.024 m²). Each
 153 gas chamber was anchored at individual 15 fixed sampling sites, but allowed to float freely on the water surface.

154 Gas was accumulating for approximately 12 h [\(each incubation had a start and end point\)](#) during [particular
 155 sampling period](#), i.e., during the day and night periods. Afterwards, 30 ml of gas was carefully taken from each
 156 chamber, after mixing the headspace in the chamber, and stored in evacuated Exetainers[®] (Labco Limited, UK).
 157 Chambers were ventilated after each sampling period to reset the incubation conditions. Methane fluxes were
 158 calculated as the difference between initial background and final concentration in the chamber headspace and
 159 expressed on the 1 m² area of the surface level per day according to Bastviken et al. (2004).

160 2.4 Background limnological parameters

161 During each campaign, [water](#) samples for analysis of nutrient concentration and phytoplankton composition were
162 collected from the surface at the deepest point using a Friedinger sampler. Water transparency was measured using
163 a Secchi [diesk](#). Total phosphorus (TP) and soluble reactive phosphorus (SRP) were analysed
164 spectrophotometrically according to Kopáček and Hejzlar (1993) and Murphy and Riley (1962), respectively.
165 Concentrations of NH_4^+ and NO_3^- were determined according to the procedure of Kopáček and Procházková
166 (1993) and Procházková (1959), respectively. Phytoplankton samples were preserved with Lugol's solution and
167 examined for species composition with an inverted microscope (Olympus IMT-2). Weather data were obtained
168 from the gauging station at the fishpond dam.

169 2.5 Statistical analyses

170 Two-tailed paired Student's t-tests and Two-way ANOVA with post-hoc Tukey's multiple comparison test (Prism
171 9.3, GraphPad Software Inc., La Jolla, USA) tested for differences between diffusive and total CH_4 fluxes between
172 day and night and among three sampling campaigns, respectively. The percentage of data variability explained by
173 different factors (daytime, month and site) was calculated with the Two-way RM ANOVA. Contour graphs
174 illustrating changes in spatial heterogeneity of measured parameters were constructed in Surfer 10 (Golden
175 Software, Inc., Colorado, USA) using the kriging contouring method. Spatial heterogeneity was quantified [for](#)
176 [each sampling](#) by calculating the spatial variance (i.e., coefficient of variation [of values measured at 15 sampling](#)
177 [sites; see, e.g. Fig 2](#)):

$$178 \text{CV\%} = 100 \times \frac{SD}{mean} \quad (7)$$

179 Higher spatial variance indicates increasing ecosystem patchiness. Linear mixed-effects models were used to
180 analyse the effects of O_2 , pH, temperature, and water depth on the CH_4 diffusive fluxes with the random effect of
181 time of day nested within the effect of sampling date. The most parsimonious model was obtained by a manual
182 backward selection, where we sequentially removed all insignificant predictors ($p > 0.05$) using likelihood ratio
183 tests implemented in the drop1 function (Zuur et al., 2009). We also compared the slopes of the month-specific
184 regression lines produced by the model using analysis of covariance (Zar, 1984). Linear mixed-effects models
185 were implemented in the lme4 package version 1.1-21 (Bates et al., 2015), and Kenward-Roger F-tests were
186 computed using the ANOVA Type II function from the pbkrtest package version 0.4-7 (Halekoh and Hojsgaard,
187 2014). The prediction of the resulting final model was visualised in the package ggeffects version 0.14.1 (Lüdecke,
188 2018). Package performance version 0.4.4 (Lüdecke et al., 2020) was used to calculate Nakagawa's R^2 of the linear
189 model. The statistical analyses were performed using R software (v. 3.5.2, R Core Team, 2018).

190 **3 Results**

191 **3.1 Weather and background fishpond characteristics**

192 Weather parameters varied among sampling campaigns. In July, clear skies prevailed with the daily air temperature
 193 above 30 °C (Table 1). During the August and September measurements, it was very cloudy, and daily air
 194 temperatures decreased to 22 and 18 °C, respectively. The water level was stable during the whole studied period
 195 with a monthly fluctuation of ~ 10 cm. Water transparency was low (15-40 cm), with an increasing trend towards
 196 the end of summer (Table 1). Concentrations of total phosphorus and soluble reactive phosphorus were high (Table
 197 1), consistent with a hyper-eutrophic state of the fishpond. In contrast, nitrogen concentrations were rather low,
 198 with ammonium nitrogen being the predominant form of inorganic N in the water (Table 1).

199 **Table 1:** Basic characteristics of the Dehtár fishpond during the studied period, [measured at the surface at the deepest point](#).

	July	August	September
Weather	Clear sky, windy	Partly cloudy, no wind	Partly cloudy, no wind
Air temperature (°C)	25-32	20-22	11-18
<u>Water temperature (°C)</u>	<u>24 - 29</u>	<u>22 - 23</u>	<u>16 - 17</u>
<u>Maximum wind speed (m s⁻¹)</u>	<u>3.2</u>	<u>0.8</u>	<u>0.9</u>
PHAR (mol m⁻² day⁻¹)	9.5	3.4	5.0
Secchi depth (cm)	15	30	40
TP (µg l⁻¹)	568	527	406
SRP (µg l⁻¹)	100	200	107
N-NH₄⁺ (µg l⁻¹)	23	783	560
N-NO₃⁻ (µg l⁻¹)	14	23	46
Chl-<i>a</i> (µg l⁻¹)	456	156	185
Phytoplankton composition	Cyanobacteria	Cyanobacteria, green algae, cryptophytes	Cryptophytes, green algae

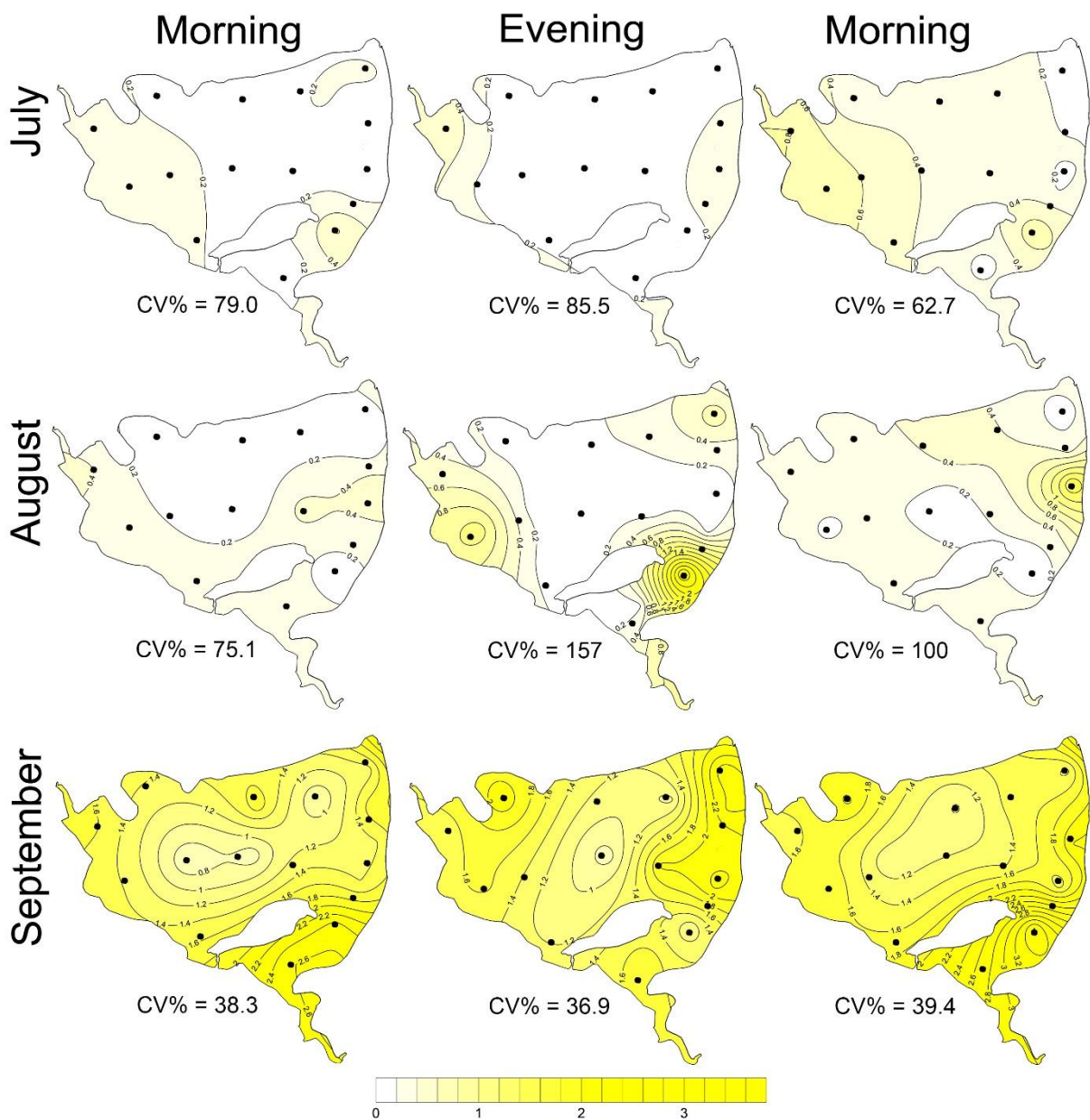
200
 201 Chlorophyll-*a* concentrations were highest in July due to the dense cyanobacterial bloom accumulated at the
 202 surface (Table 1). The phytoplankton consisted of only three cyanobacterial taxa: *Dolichospermum flos-aquae*,
 203 *Planktothrix agardhii*, and *Raphidiopsis mediteranea*. In August, phytoplankton was more diverse but also
 204 dominated by cyanobacteria: *P. agardhii*, *Aphanizomenon issatschenkoi*, and *D. flos-aquae*. In September,

205 cyanobacteria were absent and instead, cryptophytes (*Cryptomonas reflexa*), green algae (*Pediastrum*, *Coelastrum*
206 and *Desmodesmus*) and dinoflagellates (*Ceratium hirundinella*) prevailed.

207 3.2 Methane concentration and fluxes

208 The CH₄ concentration in surface water was highly supersaturated over the whole studied period. The obtained
209 values varied from 0.003 up to 3.75 μmol L⁻¹ (Fig. 2), which corresponded to saturation levels of 108-12 834%. It
210 is obvious, that the obtained data show remarkable variance: the mean (± SD) values were 0.22 ± 0.18 for July,
211 0.34 ± 0.45 for August, and 1.61 ± 0.61 μmol L⁻¹ for September (Suppl. Fig. 11).

212

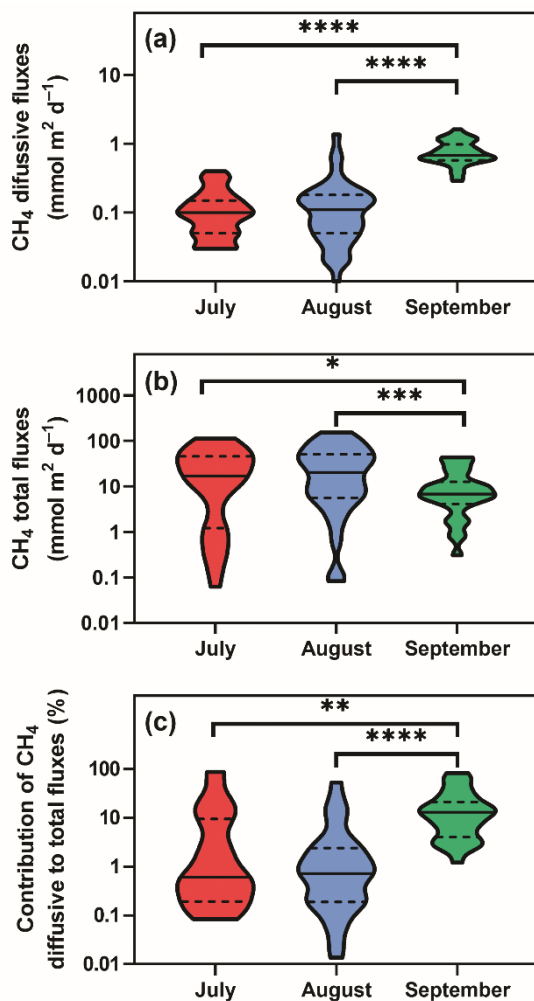


213

214 **Figure 2:** Surface methane concentrations (μmol L⁻¹). Contour graphs illustrating both seasonal and daily changes in spatial
215 heterogeneity (indicated by the coefficient of variation, CV%) in the fishpond. Black dots representing the sampling sites.

216

217 Diffusive fluxes (i.e., calculated from CH₄ concentration, see Eq. 2) showed the lowest values in July and August
218 (average 0.12 and 0.16 mmol m⁻² d⁻¹, respectively) and pronouncedly peaked in September (average 0.78 mmol
219 m⁻² d⁻¹, Fig. 3a). By contrast, in July and August, the average total CH₄ fluxes (obtained with floating chambers)
220 showed the highest values (average 31.8 mmol m⁻² d⁻¹; ranging from 0.08 to 152 mmol m⁻² d⁻¹) while in
221 September, total CH₄ fluxes were three times lower than before (average 11.8 mmol m⁻² d⁻¹, range 0.3 to 43.5
222 mmol m⁻² d⁻¹, Fig 3b). As a result, diffusive fluxes accounted for only a minor fraction of total CH₄ fluxes to the
223 atmosphere (on average, 9.2 % in July, 4.1 % in August, 18.5 % in September, Fig. 3c).



224

225 **Figure 3:** Violin plots of CH₄ diffusive (a) and total fluxes (b) during the studied period. Panel (c) depicts differences in the
226 percentage contribution of diffusive to total fluxes. Solid lines are medians, while dashed lines denote quartiles. Asterisks
227 indicate significant differences (* p<0.05, ** p<0.01, *** p<0.001, **** p<0.0001) between sampling dates determined by
228 two-way ANOVA with Tukey's multiple comparison test. Note that a log scale is used here for clarity.

229

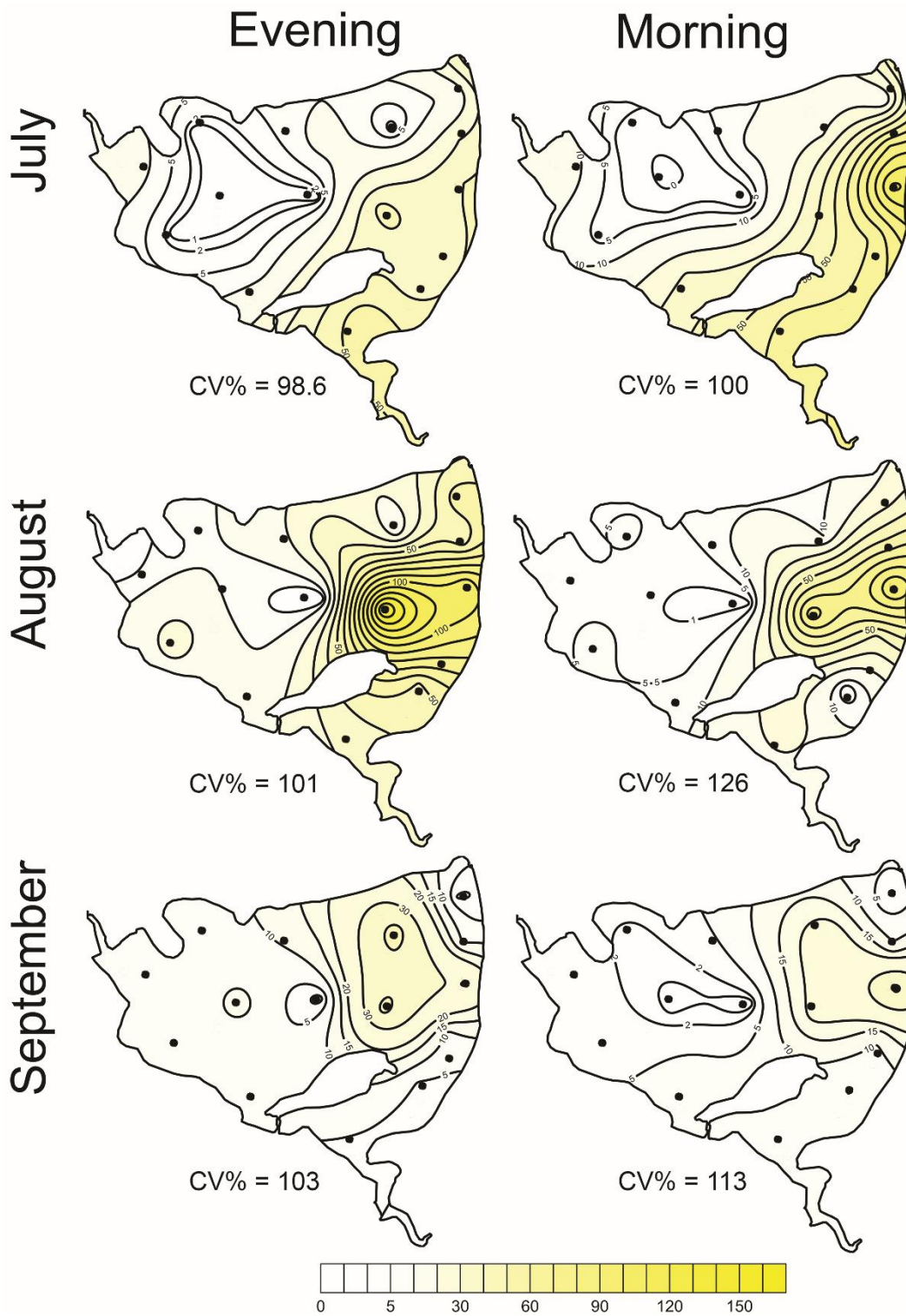
230 The total CH₄ fluxes show spatial variability within the fishpond that range ~~several~~four orders of magnitude (Fig.
231 3, 4; Suppl. Fig. 11; Suppl. Table 1). The observed spatial pattern showed high temporal variability on both daily

232 and monthly scales (Fig. 2, 4, Suppl. Table 1). Most of the variability in CH₄ diffusive fluxes was explained by
 233 sampling date (62.4 %), while for the total CH₄ fluxes, spatial heterogeneity accounted for 87.2 % of data
 234 variability (Table 2). Using linear mixed-effects models, we identified water depth as the only significant predictor
 235 of total CH₄ fluxes (Df = 1, p < 0.0001, marginal Nakagawa's R² = 0.348; Fig. 5).

236 **Table 2:** The percentage of data variability explained by different factors (daytime, month = sampling date, and site)
 237 calculated with the Two-way RM ANOVA. Statistical significant values (p < 0.01) are bold.

	% of variability				Significance		
	Daytime	Month	Site	Unexplained	Daytime	Month	Site
CH₄ diffusive flux	2.3	62.4	13.2	22.1	0.0123	<0.0001	<i>n.s.</i>
CH₄ total flux	0.19	2.4	87.2	10.2	<i>n.s.</i>	<i>n.s.</i>	<0.0001
pH	4.4	64.9	11.1	19.6	0.0001	<0.0001	<i>n.s.</i>
Water temperature	3.3	92.3	2.5	1.9	<0.0001	<0.0001	<0.0001
O₂	21.7	48.1	13.8	16.4	<0.0001	<0.0001	0.0135
Chl-<i>a</i>	0.019	74.9	16.7	8.4	<i>n.s.</i>	<0.0001	<0.0001

238 Interestingly, slopes of the linear regressions differed significantly among individual sampling campaigns (Fig. 5),
 239 indicating an additional season-related factor that affects CH₄ fluxes in the fishpond. Calculated CH₄ diffusive
 240 fluxes were not correlated with total fluxes. Linear mixed-effects models did not identify any significant predictor
 241 of the fluxes, indicating that factors and processes out of the study's scope are involved. We found no significant
 242 difference in either diffusive or total CH₄ fluxes between day and night.



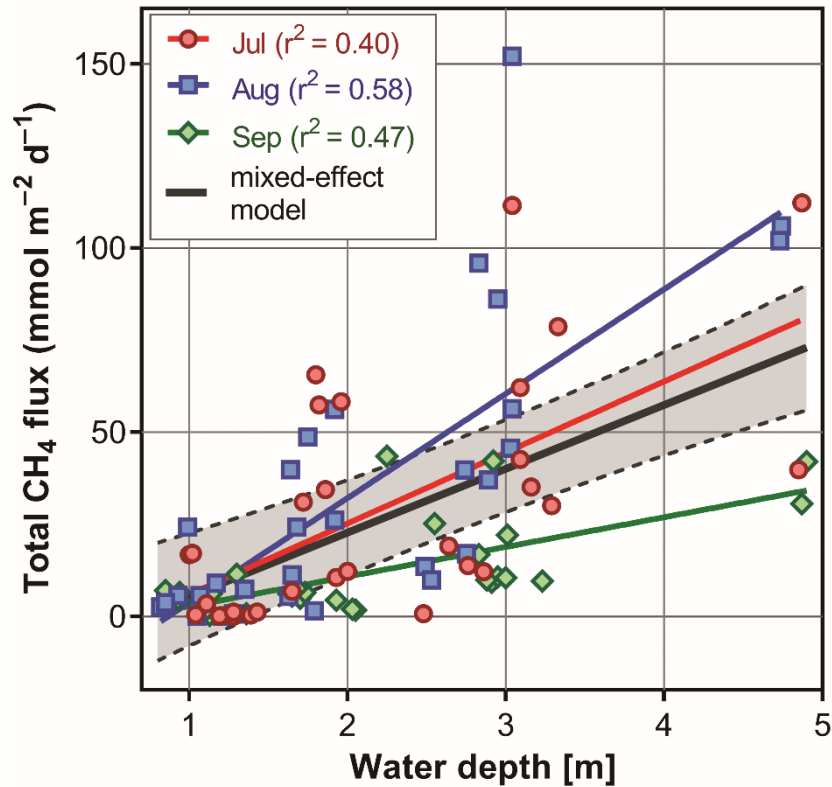
243

244

245

246

Figure 4: Contour graphs of methane total fluxes in the Dehtář fishpond. Isopleths connect sites with the same value of methane fluxes (mmol m⁻² day⁻¹). CV% is a measure of spatial heterogeneity. Black dots representing the sampling sites.

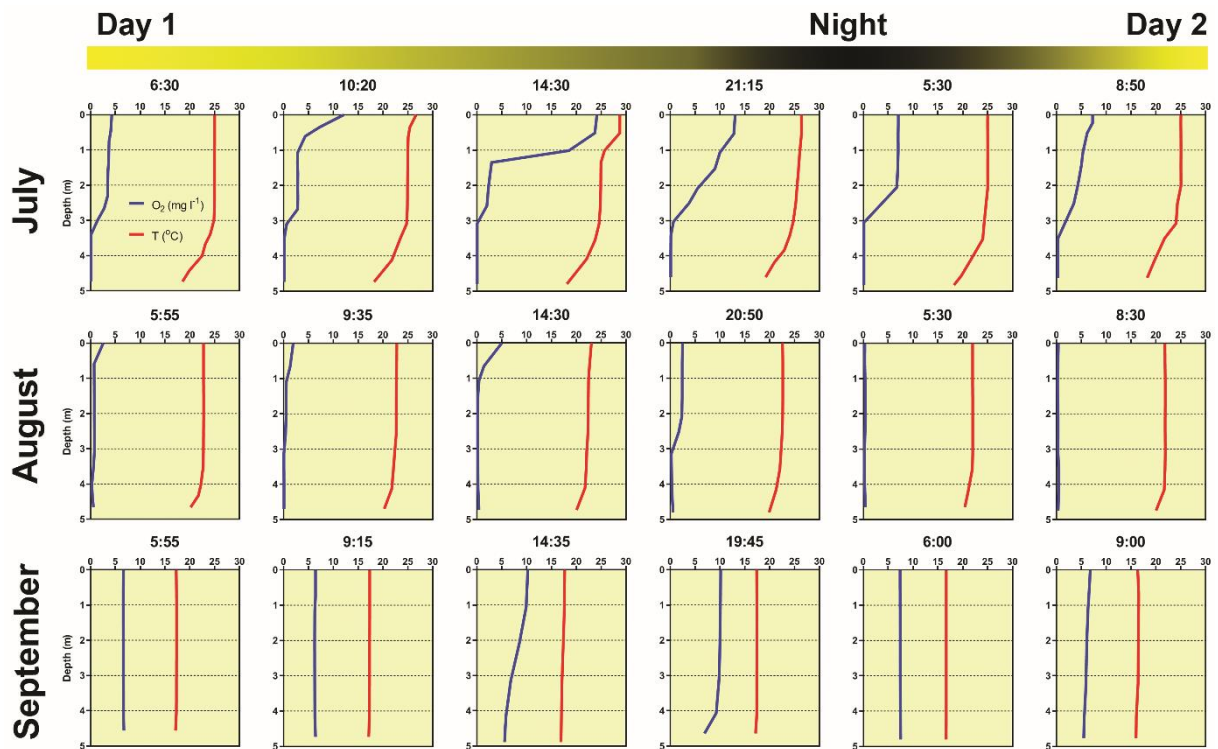


247

248 **Figure 5:** The most parsimonious linear mixed-effect model of methane total fluxes showing the water depth as the only
 249 significant predictor. Symbols are the measured values, the solid black line is the prediction, and dashed lines are 95th
 250 confidence intervals. Colours indicate month specific relation between total methane fluxes and water depth. Differences in
 251 slopes were tested using the F-test. In September, the slope of the regression line was significantly different from that in July
 252 and August.

253 3.3 Diurnal changes in vertical profiles of oxygen and temperature

254 Several contrasting patterns of vertical temperature and oxygen profiles occurred during summer 2019. Diurnal
 255 changes were most pronounced in July (Fig. 6). Surface temperatures varied from 25 °C in the morning to nearly
 256 30 °C in the afternoon. Thermal stratification of the water column was weak in the morning but became strongest
 257 at 14:30 with a thermocline at 0.5 m depth (Fig. 6). Later in the afternoon, the water column began to be mixed by
 258 wind. The morning vertical oxygen profile was characterised by a surface value of 4.3 mg L⁻¹, corresponding to
 259 51 % saturation and anoxia below 3 m.



260

261 **Figure 6:** Diurnal changes in vertical profiles of temperature and oxygen concentration measured at the deepest point of the
 262 fishpond. Numbers above each graph indicate the time of measurement.

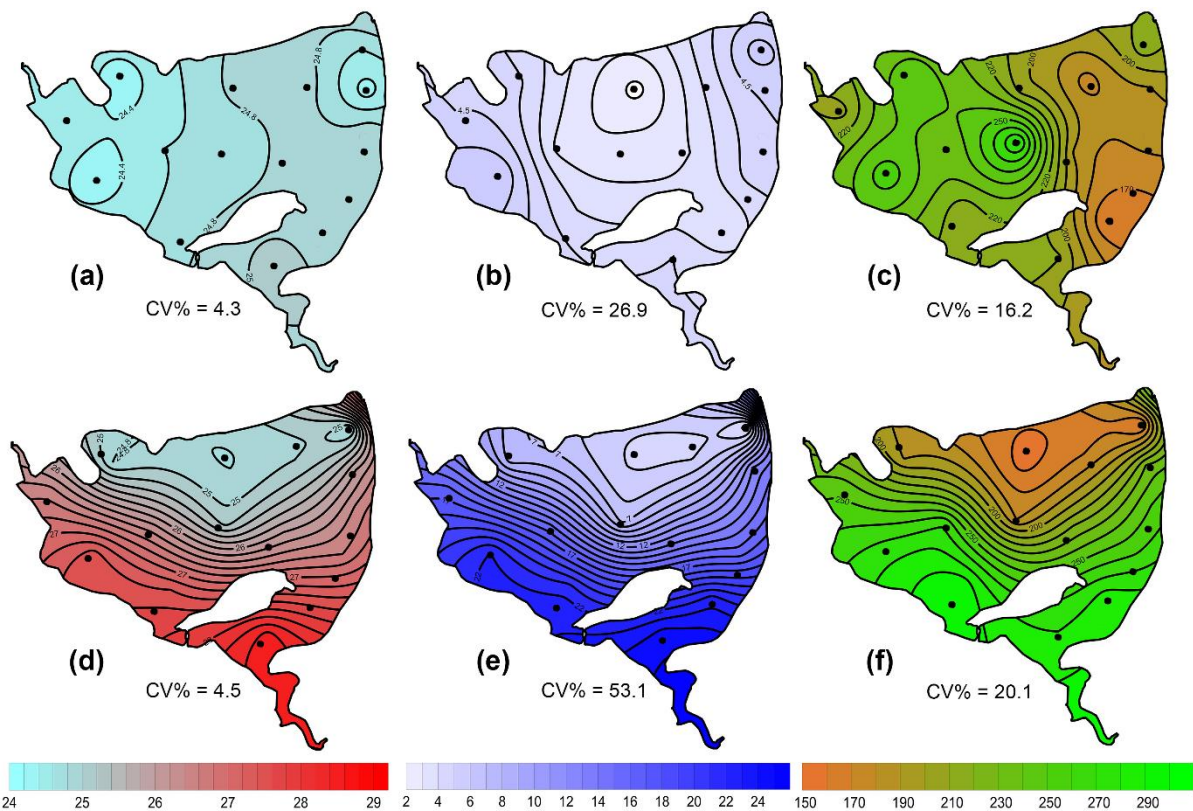
263 Due to the high photosynthetic activity of cyanobacteria, the surface oxygen concentration increased to 24 mg L^{-1}
 264 1 (320 % saturation, Fig. 6), and a steep oxycline was established at a depth of 0.5-1.5 m with no effect on the
 265 anoxic conditions at the deeper layers. Wind action eroded both the oxy- and thermoclines in the evening, and by
 266 the next morning, the vertical profiles were similar to those at the beginning.

267 In August, the water column was almost entirely mixed and low in oxygen in the morning, with only 2.6 mg L^{-1}
 268 (30 % saturation) of oxygen at the surface. Due to cloudy weather, the daily photosynthetic activity of
 269 phytoplankton resulted in only a slight increase in oxygen concentration at 0-1.5 m depth (4 mg L^{-1} , 47 %
 270 saturation). By the morning of the next day, the entire water column turned very close to anoxic (0.4 mg L^{-1} , 4 %
 271 saturation; Fig. 6), which in turn affected the spatial distribution of zooplankton, as evidenced by the formation of
 272 dense zooplankton clouds accumulated in the thin layer just at the surface (see Suppl. Fig. 3). In September, the
 273 water column was completely mixed, and we observed only weak daily changes in thermal and oxygen vertical
 274 structures (Fig. 6).

275 3.4 Effect of wind on spatial heterogeneity of temperature, oxygen and chlorophyll-*a*

276 During the summer, all measured parameters showed remarkable within-lake spatial heterogeneity (Suppl. Fig. 5-
 277 8). In July, meteorological conditions allowed for demonstrating the effect of wind on fishpond spatial

278 heterogeneity. In the morning, there were no substantial differences in the surface temperature and oxygen
 279 concentrations (Fig. 7ab). Phytoplankton biomass was accumulated mostly in the shallow western part, with the
 280 maximum in the centre (Fig. 7c). At 14:00, a light breeze started to blow from the northwest, achieving a maximum
 281 of ~~11.3.2 km sh~~^{11.3.2 km sh}⁻¹ (Suppl. Fig. 9). This episode lasted till the evening measurement, and the wind ceased by 21:00.
 282 The wind was strong enough to change spatial distribution substantially (Fig. 7d-f, Suppl. Fig. 4). In the evening,
 283 the surface water temperature on the windward (south) side of the fishpond was ~ 4 °C higher than in the north
 284 (Fig. 7d). The wind also induced order of magnitude differences in oxygen concentration along the north-south
 285 axis of the fishpond (3 mg L⁻¹ of O₂ at the north, 24 mg L⁻¹ of O₂ at the south; Fig. 7e) and affected phytoplankton
 286 distribution in the fishpond, resulting in remarkable bloom accumulation in the south (Fig. 7f, Suppl. Fig. 8).
 287 During the calm night after the disturbance, the north-south gradient substantially weakened. In August and
 288 September, the thermal heterogeneity of the pond was rather low, but the spatial distribution of oxygen and
 289 chlorophyll-a remained highly variable (Suppl. Fig. 5–8, Suppl. Table 1).



290
 291 **Figure 7:** Contour graphs of surface temperature (a, d; °C), oxygen concentration (b, e; mg L⁻¹) and chlorophyll-a
 292 concentration (c, f; µg L⁻¹) measured on July 2 at different times of day: a, b and c are the morning measurements; d, e and f
 293 are evening measurements following a wind disturbance. Coefficient of variation (CV %) is a measure of spatial heterogeneity
 294 of measured parameters. Black dots representing the sampling sites.

295 **Discussion**

296 **4.1 Methane fluxes**

297 Assessing spatial heterogeneity of the CH₄ fluxes within a fishpond is critical for a reliable estimate of its
298 contribution to the global CH₄ budget. In our study, the variability in total CH₄ fluxes spanned several orders of
299 magnitude (ranging from 0.06 up to 1 121.3 mmol m⁻² d⁻¹), which is in agreement with similar studies (Casper et
300 al., 2000; DelSontro et al., 2016; Natchimuthu et al., 2016). However, most system-specific CH₄ flux estimates rely
301 on upscaling from a limited number of sites (Bastviken et al., 2004; Rasilo et al., 2015; Wik et al., 2016) because
302 obtaining spatial variability in CH₄ emission is methodologically challenging. In general, spatial heterogeneity
303 may reflect differences in water sources, physical mixing, local transformations and biogeochemical processes and
304 rates among lake habitats (Loken et al., 2019). In deep lakes, littoral areas can contribute disproportionately to
305 total lake CH₄ fluxes (Hofmann et al., 2010; Hofmann 2013, Natchimuthu et al., 2016; Schilder et al., 2013) and
306 are often missed by traditional sampling approaches (Wik et al., 2016). According to Wik et al. (2016), low
307 temporal and spatial resolutions are unlikely to cause overestimates. On the other hand, DelSontro et al. (2018b)
308 suggested that horizontal transport of CH₄ produced in littoral zones and the interaction between physical and
309 biological processes (e.g. air-water gas exchange, water column mixing, the interplay between CH₄ production
310 and microbial oxidation) may result in an underestimation of whole-lake CH₄ fluxes based on centre samples.
311 Similarly, Natchimuthu et al. (2016) found that up to 78 % underestimation would occur if samples obtained only
312 from the lake center are used to extrapolate the total CH₄ flux. However, extrapolating our data from the deepest
313 point of the Dehtář fishpond would lead to an overestimation of the CH₄ fluxes by a factor of 2.9 (Suppl. Fig. 12).
314 The bias introduced by the deepest point measurement appears to be highly variable among systems with different
315 morphology, geographical location, mixing regimes or trophic states. For instance, analysis of 22 European lakes
316 during late summer has shown that spatially resolved CH₄ diffusive fluxes were highly variable for individual
317 lakes, yielding 55–300 % differences in the whole-lake estimates (Schilder et al., 2013). Schmiedeskamp et al.
318 (2021) observed an increase in CH₄ fluxes from the shore towards the centre in response to increasing sediment
319 C-content in two shallow German lakes. In line with these findings, our results provide further evidence that
320 spatially resolved data are needed to validate the uncertainties that come from using single-point samples to
321 represent whole-lake processes in hyper-eutrophic systems. As stated by Loken et al. (2019), rather than assuming
322 spatial homogeneity, scaling-up exercises of global carbon budgets should acknowledge the uncertainty that comes
323 from extrapolating from spatially limited data sets.

324 In the Dehtář fishpond, the total CH₄ fluxes increased with water depth, and this relationship was month specific.
325 The highest CH₄ fluxes at the deepest points may seem contradictory to previous studies, in which the highest
326 fluxes were typically observed in littoral areas (e.g. DelSontro et al., 2018b; Hofman et al., 2010; Natchimuthu et
327 al., 2016; Schilder et al., 2013). However, these findings are based on studying mostly lakes whose morphology,
328 trophic state or oxygen regime sharply contrast with the Dehtář fishpond, where the upper two meters of the water
329 column were oxygen-saturated while the deepest strata were mostly anoxic. i.e. the extent and duration of bottom
330 anoxia could be the most influential factor contributing to the highest methane fluxes at the deepest point of the
331 pond. In such hyper-eutrophic systems, high nutrient loading increases autochthonous primary production
332 (Potužák et al., 2007; Rutegwa et al., 2019) and promotes oxygen consumption and anaerobic decomposition in
333 the sediments (Baxa et al., 2020), leading to enhanced CH₄ production (Bastviken et al., 2004; Grasset et al., 2018).
334 In aquaculture ponds in Southeast China, CH₄ fluxes exhibited considerable spatial variations and peaked in the
335 relatively deep feeding zone, where the large loads of sediment organic matter fueled CH₄ production (Yang et al.,
336 2020). Furthermore, sediment temperature was the strongest predictor of CH₄ fluxes in ponds (DelSontro et al.,
337 2016; Yang et al., 2020). It is, therefore, reasonable to assume that both temperature and oxygen concentration in
338 the sediment likely contributed to changes in observed CH₄ fluxes during the studied period in our study. Although
339 both parameters were not directly measured in the sediment, it can be deduced from their vertical profiles that the
340 probability of sediment anoxia was highest in August and lowest in September, and the sediment temperature was
341 lowest in September (see Fig. 5).

342 Our results agree with the generally accepted view that processes other than diffusive fluxes – most likely
343 ebullition – represent the major CH₄ pathway to the atmosphere in hyper-eutrophic ponds (Kosten et al., 2020).
344 Although freshwaters with high primary production are more likely to have high CH₄ ebullition rates (DelSontro
345 et al., 2016), the dominant role of ebullition was also found across lentic systems differing in size, trophic status
346 or geographical location (Aben et al., 2017). Ebullition accounted on average for 56 % of total CH₄ fluxes in
347 northern ponds in Canada (DelSontro et al., 2016), 49 and 71 % in two different zones of Lake Taihu (Xiao et al.,
348 2017) and 48-83 % in three Swedish lakes (Natchimuthu et al., 2016; Jansen et al., 2019). The highest contribution
349 was found in the small hyper-eutrophic Priest Pot (UK), where ebullition represented 96 % of the total CH₄ flux
350 from the pond (Casper et al., 2000). Apparently, the contribution of ebullition can vary among systems and will
351 remain uncertain until measurement designs cover enough spatiotemporal variability to yield representative values
352 for the whole ecosystem.

353 In shallow water bodies, a semi-stable flux of microbubbles was suggested to account for a significant portion of
354 the total CH₄ flux (Prairie and del Giorgio, 2013). When CH₄ concentration in the water column is above a certain
355 threshold of microbubble density, these microbubbles likely aggregate, fuse, and escape to the atmosphere from
356 buoyancy (Prairie and del Giorgio, 2013). Even a small fluctuation in hydrostatic pressure (e.g., due to changes in
357 atmospheric pressure) or lake water level was shown to trigger enhanced CH₄ ebullition (Bastviken et al., 2004;
358 Casper et al., 2000; Varadharajan and Hemond, 2012). Since ebullition rates increase exponentially with
359 temperature, CH₄ fluxes tend to peak in warm summer months (van Bergen et al., 2019). In our study, 1 % lower
360 air pressure in July and August than in September, along with bottom anoxia and higher water temperature, could
361 account for the enhanced release of CH₄ bubbles from the sediment (31.7 mmol m⁻²d⁻¹, >90 % of total CH₄ fluxes;
362 Suppl. Fig. 2). In September, when we observed the lowest water temperatures from the studied period and the
363 oxygen profile was rather uniform, ebullition accounted for 81 % (11 mmol m⁻²d⁻¹) of the total CH₄ fluxes. The
364 spatially pooled data of the total CH₄ fluxes measured in the Dehtář fishpond varied from 11.8 to 34.5 mmol m⁻²
365 d⁻¹, which is comparable with similar systems elsewhere (e.g., Bastviken et al., 2010; van Bergen et al., 2019;
366 Baron et al., 2022). To sum up, both diffusive fluxes and ebullition must be addressed to understand the magnitude
367 of total aquatic CH₄ fluxes and how their relative contributions vary across and within aquatic systems (Kosten et
368 al., 2020). Moreover, with an improved determination of CH₄ hot-spots and its causes, the management of ponds
369 could be changed accordingly and so the overall emissions reduced for example by decreasing P-availability and
370 dredging (Nijman et al., 2022).

371 **4.2 Effect of wind event on ecosystem spatial structure**

372 Sudden changes in ecosystem spatial structure in response to meteorological forcing have rarely been documented
373 (Loken et al., 2019) since they are hard to predict. Research into them using traditional methods requires intensive
374 effort or expensive instrumentation (Ortiz and Wilkinson, 2021), and it remains a matter of luck to obtain a relevant
375 dataset. In the July sampling campaign, we observed a strong impact of the wind on environmental heterogeneity
376 in the fishpond, which was apparent at a sub-daily time scale. Due to the methodological constraints, i.e., lack of
377 initial measurement, we can only speculate about the effect of wind on the total CH₄ fluxes. The northwest wind
378 during the day advected warmed surface water with cyanobacterial bloom from the north basin to the south. In the
379 evening, it resulted in bloom accumulation on the upward side and a north-south gradient of more than 4 °C and
380 4-24 mg L⁻¹ oxygen. After the winds fell off, the observed gradients declined during cooling at night. We assume
381 that the wind blowing across the pond surface drove buoyant cyanobacteria and surface water downwind and
382 caused an upwelling of deeper, colder, and hypoxic water on the upwind side. This wind-related circulation pattern

383 has been described as a “conveyer belt” in classical textbooks (Reynolds et al., 2006), held responsible for a
384 disruption of the thermal structure of the water column and the non-uniform spatial distribution of pH, oxygen,
385 CO₂ or CH₄ and also plankton assemblages (e.g. Loken et al., 2019; Natchimuthu et al., 2016; Rinke et al., 2009;
386 Ortiz and Wilkinson, 2021).

387 Similar to our study, mild winds (~4 m s⁻¹) were strong enough to redistribute heat and induce lake-wide
388 circulations driving upwelling and downwelling in 24 m deep Lake Pleasant (Czikowsky et al., 2018). As the wind
389 blows harder and lasts longer, the effects on ecosystem functioning may target higher trophic levels and become
390 more complex (Rinke et al., 2009). In Lake Constance, a three day storm event with wind velocities of ~10 m s⁻¹
391 resulted in a lake-wide displacement of water masses and the formation of the 6-15 °C horizontal surface water
392 gradient, which in turn changed the spatial distribution of phytoplankton, zooplankton and juvenile fish (Rinke et
393 al., 2009). After several stormy days (wind velocities of 12-15 m s⁻¹), Čech et al. (2011) observed negative effects
394 of wind-driven changes in water temperature and wave action on perch (*Perca fluviatilis*) spawning in the Lake
395 Milada. Although wind events affect shallow and deep lakes differently, there is growing evidence that they can
396 have far-reaching consequences on the functioning of aquatic ecosystems by disrupting energy flows, nutrient
397 fluxes, productivity and reproduction, and consequently altering community composition and trophic interactions
398 in the short and long term (Stockwell et al., 2020). As the frequency, intensity, spatial extent and duration of these
399 extreme meteorological events are projected to increase due to ongoing climate change (Comou and Rahmstorf,
400 2012), there is an urgent need to better understand the mechanisms underlying their impacts on the maintenance
401 of the ecosystem services.

402 **4.3 Summer changes in the oxygen regime**

403 Our data demonstrate that shallow, hyper-eutrophic ponds have disrupted oxygen regimes (Baxa et al., 2021) with
404 anoxic hypolimnion and may experience severe whole-water column hypoxia critical for aquatic biota (Miranda
405 et al., 2001). The hypoxic periods may result, for example, from sudden weather change (Jeppesen et al., 1990)
406 and last several days, during which physical processes and phytoplankton photosynthesis cannot compensate for
407 intense community respiration (Baxa et al., 2021). This became obvious in August when severe oxygen depletion
408 was measured at the surface across the whole pond, mostly far below a critical level of 4.5 mg L⁻¹, when adverse
409 effects came into play (Banerjee et al., 2019). However, oxygen surface concentrations in shallow parts of the
410 pond were substantially higher regardless of the time of day, which contrasts with findings of Miranda et al. (2001),
411 who emphasised shallow waters as the most sensitive parts of lakes, where hypoxic events can occur due to the
412 respiration of sediment biota. The observed spatial gradients of oxygen may create temporal refugia which allow

413 fish to survive harsh conditions that occur in the deepest part of the pond. To minimise economic losses and
414 negative impacts on the ecosystem, future research should identify the interplay between meteorological forcing,
415 trophic status and anthropogenic pressures (e.g. management practices) that affect oxygen fluctuations at various
416 time scales.

417 **4.4 Study limitations**

418 Like in other research, there are some limitations in the current study. Since our measurement had only a limited
419 temporal resolution (three samplings during the summer season), it is not appropriate to extrapolate CH₄ emissions
420 for annual values. Noticeably, future research must increase the frequency of the sampling and include also
421 innovative techniques to measure CH₄ fluxes at multiple fishponds, with different management regime. In our
422 study, the 12 h deployment time of the floating chambers could have led to extensive gas accumulation, which in
423 turn might have resulted in an underestimation of the total CH₄ fluxes due to the dissolution of the CH₄ from the
424 chamber into the water once the equilibrium concentration in the chamber is overcome (Bastviken et al., 2010).
425 However, CH₄ concentrations in water corresponded to a supersaturation of several orders of magnitude, so the
426 introduced bias appears to be of minor importance. In any case, our daily CH₄ fluxes represent a rather conservative
427 estimate for the global methane budget. In our study, we also did not address the important processes that could
428 shed light on the lake CH₄ budget, such as CH₄ oxidation rates (Bastviken et al., 2008) or biological interaction
429 (e.g. protistan grazing on CH₄ oxidising bacteria) in aquatic food webs (Sanseverino et al., 2012) that can affect
430 the overall CH₄ fluxes. We also lack information about spatial differences in sediment microbiota and organic
431 carbon content and compositions, which were found to affect CH₄ production rates (Berberich et al., 2020;
432 Emerson et al., 2021). Despite the limitation mentioned above, our results show that complementary spatial
433 surveys help contextualise the fixed station dynamics and provide additional, management-relevant information
434 about the fishpond.

435 For improved monitoring strategies, however, a continuous measurement approach like eddy covariance would be
436 generally more efficient than traditional sampling at regular intervals. Eddy covariance accounts for temporal
437 variability and provides high temporal resolution data by continuously measuring wind speed, gas concentration,
438 and vertical turbulent fluxes to estimate methane emissions (Erkillä et al., 2018). More importantly, it also offers
439 spatially integrated measurements, averaging emissions over a larger area and therefore accounts for pond spatial
440 heterogeneity. However, it's worth noting that the choice of monitoring approach depends on various factors,
441 including the specific objectives, available resources, and the characteristics of the emission sources. To accurately
442 capture both short-term variability and lake spatial heterogeneity of methane ebullition and diffusion fluxes, the

443 most efficient approach was found to be a combination of continuous measurements with traditional methods
444 including floating chambers, anchored funnels and boundary model calculations (Schubert et al., 2012, Podgrajsek
445 et al., 2014, Erkillä et al., 2018). This integrated approach would provide a comprehensive understanding of
446 methane emissions, enabling better estimation and more effective mitigation efforts.

447 **5. Conclusions**

448 Deciphering the mechanisms that drive spatial and temporal heterogeneity in aquatic ecosystem structure and
449 function not only expands our understanding of pond ecology but also provides insights to improve the
450 management of these ecosystems and the services they provide. Our results suggest that spatial heterogeneity needs
451 to be considered when designing experiments and monitoring programs. Without the spatially resolved sampling,
452 we introduce bias into our datasets, hampering our limnological understanding of the ecosystem's functioning and
453 impeding our ability to accurately estimate rates such as methane emissions on a global scale (DelSontro et al.,
454 2018a). In agreement with Kosten et al. (2020), we demonstrated that neglecting ebullition leads to a considerable
455 underestimating of the total CH₄ fluxes. Since there are thousands of these intensively managed fishponds, we
456 argue for changing the management practices toward sustainable use of natural resources to mitigate the overall
457 emissions of greenhouse gases from these ecosystems. Future studies are needed to characterise CH₄ fluxes over
458 a greater number and diversity of aquaculture ponds and examine the mechanisms controlling CH₄ emissions in
459 aquatic ecosystems.

460 **Acknowledgements**

461 The study was supported by the Czech Science Foundation (Research Projects No. 17-09310S, 19-23261S and
462 P504/19-16554S). We thank Dr. Martin Rulík for providing us gas chambers. We especially thank to Prof.
463 Miloslav Šimek and Linda Jiřová for enabling gas analyses. We are grateful Anna Sieczko for consultation on the
464 calculation of CH₄ fluxes. English correction was made by Anton Baer.

465 **Data availability**

466 Dataset associated with the manuscript can be found in the GitHub Repositories under
467 <https://zenodo.org/badge/latestdoi/587640213>.

468 **Author contributions**

469 All authors contributed to the study conception and design. PZ planned the campaign; PZ, AM and JN performed
470 the sampling and analyzed the data; AM performed the gas-measurements; VK performed statistical analyses and
471 modelling; PZ and AM wrote the manuscript. All authors read and approved the final manuscript.

472 **References**

- 473 Aben, R.C.H., Barros, N., van Donk, E., Frenken, T., Hilt, S., Kazanjian, G., Lamers, L.P.M., Peeters, E.T.H.M.,
474 Roelofs, J.G. M, de Senerpont Domis, L.N., Stephan, S., Velthuis, M., Van de Waal, D.B., Wik, M., Thornton,
475 B.F., Wilkinson, J., DelSontro, T., and Kosten, S.: Cross continental increase in methane ebullition under climate
476 change. *Nat. Commun.*, 8, 1682, <https://doi.org/10.1038/s41467-017-01535-y>, 2017.
- 477 Banerjee, A., Chakrabarty, M., Rakshit, N., Bhowmick, A.R., and Ray, S.: Environmental factors as indicators of
478 dissolved oxygen concentration and zooplankton abundance: deep learning versus traditional regression approach.
479 *Ecol. Indic.*, 100, 99-117, <https://doi.org/10.1016/j.ecolind.2018.09.051>, 2019.
- 480 Baron, A.A.P., Dyck, L.T., Amjad, H., Bragg, J., Kroft, E., Newson, J., Oleson, K., Casson, N.J., North, R.L.,
481 Venkiteswaran, J.J., and Whitfield, C.J.: Differences in ebullitive methane release from small, shallow ponds
482 present challenges for scaling. *Sci. Total Environ.*, 802, 149685, <https://doi.org/10.1016/j.scitotenv.2021.149685>,
483 2022.
- 484 Bartosiewicz, M., Maranger, R., Przytulska, A., and Laurion, I.: Effects of phytoplankton blooms on fluxes and
485 emissions of greenhouse gases in a eutrophic lake. *Water Res.*, 196, 116985,
486 <https://doi.org/10.1016/j.watres.2021.116985>, 2021.
- 487 Bastviken, D., Cole, J., Pace M., and Tranvik, L.: Methane emissions from lakes: Dependence of lake
488 characteristics, two regional assessments, and a global estimate. *Global Biogeochem. Cycles*, 18, GB4009,
489 <https://doi.org/10.1029/2004GB002238>, 2004.
- 490 Bastviken, D., Cole, J.J., Pace, M.L., and Van de Bogert, M.C.: Fates of methane from different lake habitats:
491 connecting whole-lake budgets and CH₄ emissions. *J. Geophys. Res. Biogeosci.*, 113, G02024,
492 <https://doi.org/10.1029/2007JG000608>, 2008.
- 493 Bastviken, D., Santoro, A.L., Marotta, H., Pinho, L.Q., Calheiros, D.F., Crill, P., and Enrich-Prast, A.: Methane
494 Emissions from Pantanal, South America, during the Low Water Season: Toward More Comprehensive Sampling.
495 *Environ. Sci. Tech.*, 44, 5450-5455, <https://doi.org/10.1021/es1005048>, 2010.
- 496 Bates, D., Maechler, M., Bolker, B., and Walker, S.: Fitting Linear Mixed-Effects Models Using lme4. *J. Stat.*
497 *Soft.*, 67, 1-48, <https://doi.org/10.18637/jss.v067.i01>, 2015.
- 498 Baxa, M., Musil, M., Kummel, M., Hazlík, O., Tesařová, B., and Pechar, L.: Dissolved oxygen deficits in a shallow
499 eutrophic aquatic ecosystem (fishpond) – Sediment oxygen demand and water column respiration alternately drive
500 the oxygen regime. *Sci. Total Environ.*, 766, 142647, <https://doi.org/10.1016/j.scitotenv.2020.142647>, 2021.
- 501 ~~Beaulieu, J.J., DelSontro, T., and Downing, J.A.: Eutrophication will increase methane emissions from lakes and~~
502 ~~impoundments during the 21st century. *Nat. Commun.*, 10, 3-7, <https://doi.org/10.1038/s41467-019-09100-5>,~~
503 ~~2019.~~

504 Berberich, M.E., Beaulieu, J.J., Hamilton, T.L., Waldo, S., and Buffam, I.: Spatial variability of sediment methane
505 production and methanogen communities within a eutrophic reservoir: Importance of organic matter source and
506 quantity. *Limnol. Oceanogr.*, 65, 1336-1358, <https://doi.org/10.1002/lno.11392>, 2020.

507 Bižić, M., Klintzsch, T., Ionescu, D., Hindiyeh, M.Y., Günthel, M., Muro-Pastor, A.M., Eckert, W., Ulrich, T.,
508 Keppler, F., and Grossart, H.P.: Aquatic and terrestrial cyanobacteria produce methane. *Sci. Adv.*, 6, 1-10,
509 <https://doi.org/10.1126/sciadv.aax5343>, 2020.

510 Bussmann, I., Matoušů, A., Osudar, R., and Mau, S.: Assessment of the radio $^3\text{H-CH}_4$ tracer technique to measure
511 aerobic methane oxidation in the water column. *Limnol. Oceanogr.- Meth.*, 13, 312-327,
512 <https://doi.org/10.1002/lom3.10027>, 2015.

513 Casper, P., Maberly, S.C., Hall, G.H., and Finlay, B.J.: Fluxes of methane and carbon dioxide from a small
514 productive lake to the atmosphere. *Biogeochemistry*, 49, 1-19, <https://doi.org/10.1023/A:1006269900174>, 2000.

515 Čech, M., Peterka, J., Říha, M., Muška, M., Hejzlar, J., and Kubečka, J.: Location and timing of the deposition of
516 eggs strands by perch (*Perca fluviatilis* L.): the roles of lake hydrology, spawning substrate and female size.
517 *Knowl. Manag. Aquat. Ecosyst.*, 403, 1-12, <https://doi.org/10.1051/kmae/2011070>, 2011.

518 Céréghino, R., Biggs, J., Oertli, B., and Declerck, S.: The ecology of European ponds: defining the characteristics
519 of a neglected freshwater habitat. *Hydrobiologia*, 597, 1-6, <https://doi.org/10.1007/s10750-007-9225-8>, 2008.

520 Coumou, D. and Rahmstorf, S.: A decade of weather extreme. *Nat. Clim. Change*, 2, 491-96,
521 <https://doi.org/10.1038/nclimate1452>, 2012.

522 Crusius, J. and Wanninkhof, R.: Gas transfer velocities measured at low wind speed over a lake. *Limnol. Oceanogr.*,
523 48, 1010-1017, <https://doi.org/10.4319/lo.2003.48.3.1010>, 2003.

524 Czikowsky, M.J., MacIntyre, S., Tedford, E.W., Vidal, J., and Miller, S.D.: Effects of wind and buoyancy on
525 carbon dioxide distribution and air-water flux of a stratified temperate lake. *J. Geophys. Res. Biogeosci.*, 123,
526 2305-2322, <https://doi.org/10.1029/2017JG004209>, 2018.

527 De Meester, L., Declerck, S., Stoks, R., Louette, G., Van de Meutter, F., De Bie, T., Michels, E., and Brendonck,
528 L.: Ponds and pools as model systems in conservation biology, ecology and evolutionary biology. *Aquat. Cons.*,
529 15, 715-725, <https://doi.org/10.1002/aqc.748>, 2005.

530 DelSontro, T., Boutet, L., St-Pierre, A., del Giorgio, P.A., and Prairie, Y.T.: Methane ebullition and diffusion from
531 northern ponds and lakes regulated by the interaction between temperature and system productivity. *Limnol.*
532 *Oceanogr.*, 61, 62-77, <https://doi.org/10.1002/lno.10335>, 2016.

533 DelSontro, T., Beaulieu, J.J., and Downing, J.J.: Greenhouse gas emissions from lakes and impoundments:
534 upscaling in the face of global change. *Limnol. Oceanogr. Lett.*, 3, 64-75, <https://doi.org/10.1002/lo12.10073>,
535 2018a.

536 DelSontro, T., del Giorgio, P.A., and Prairie, Y.T.: No Longer a Paradox: The Interaction Between Physical
537 Transport and Biological Processes Explains the Spatial Distribution of Surface Water Methane Within and Across
538 Lakes. *Ecosystems*, 21, 1073-1087, [10.1007/s10021-017-0205-1](https://doi.org/10.1007/s10021-017-0205-1), 2018b.

539 Emerson, J.B., Varner, R.K., Wik, M., Parks, D.H., Neumann, R.B., Johnson, J.E., Singleton, C. M., Woodcroft,
540 B.J., Tollerson II, R., Owusu-Dommey, A., Binder, M., Freitas, N. L., Crill, P.M., Saleska, S.R., Tyson, G.W., and
541 Rich, V.I.: Diverse sediment microbiota shape methane emission temperature sensitivity in Arctic lakes. *Nat.*
542 *Commun.*, 12, 5815, <https://doi.org/10.1038/s41467-021-25983-9>, 2021.

543 [Erkkilä, K.-M., Ojala, A., Bastviken, D., Biermann, T., Heiskanen, J. J., Lindroth, A., Peltola, O., Rantakari, M.,](#)
544 [Vesala, T., and Mammarella, I.: Methane and carbon dioxide fluxes over a lake: comparison between eddy](#)
545 [covariance, floating chambers and boundary layer method, Biogeosciences, 15, 429–445,](#)
546 <https://doi.org/10.5194/bg-15-429-2018>, 2018.

547 Grasset, Ch., Mendonça, R., Saucedo, G.V., Bastviken, D., Roland, F., and Sobek, S.: Large but variable methane
548 production in anoxic freshwater sediment upon addition of allochthonous and autochthonous organic matter.
549 *Limnol. Oceanogr.*, 63, 1488-1501, <https://doi.org/10.1002/lno.10786>, 2018.

550 Halekoh, H. and Hojsgaard, S.: A Kenward-Roger Approximation and Parametric Bootstrap Methods for Tests in
551 Linear Mixed Models - The R Package pbrtest. *J. Stat. Soft.*, 59, 1-30, <https://doi.org/10.18637/jss.v059.i09> 2014.

552 Hofmann, H., Federwisch, L., and Peeters, F.: Wave-induced release of methane: littoral zones as a source of
553 methane in lakes. *Limnol. Oceanogr.*, 55, 1990-2000, <https://doi.org/10.4319/lo.2010.55.5.1990>, 2010.

554 Hofmann, H.: Spatiotemporal distribution patterns of dissolved methane in lakes: How accurate are the current
555 estimations of the diffusive flux path? *Geophys. Res. Lett.*, 40, 2779-2784, <https://doi.org/10.1002/grl.50453>,
556 2013.

557 Hu, Z., Wu, S., Ji, Ch., Zou, J., Zhou, Q., and Liu, S.: A comparison of methane emissions following rice paddies
558 conversion to crab-fish farming wetlands in southeast China. *Environ. Sci. Pollut. Res.*, 23, 1505-1515,
559 <https://doi.org/10.1007/s11356-015-5383-9>, 2016.

560 Jansen, J., Thornton, B.F., Jarnet, M.M., Wik, M., Cortés, A., Friberg, T., MacIntyre, S., and Crill, P.M.:
561 Climate-sensitive controls on large spring emissions of CH₄ and CO₂ from northern lakes. *J. Geophys. Res.*,
562 *Biogeosciences*, 124, 2379-2399, <https://doi.org/10.1029/2019JG005094>, 2019.

563 [Jähne, B., Münnich, K. O., Börsinger, R., Dutzi, A., Huber, W., and Libner, P.: On the parameters influencing air-](#)
564 [water gas exchange, J. Geophys. Res., 92, C2, 1937-1949, doi:10.1029/JC092iC02p01937, 1987.](#)

565 Jeppesen, E., Søndergaard, M., Sortkjaer, O., Mortensen, E., and Kristensen, P.: Interactions between
566 phytoplankton zooplankton and fish in a shallow hypertrophic Lake a study of phytoplankton collapses in Lake
567 Sobygaard, Denmark. *Hydrobiologia*, 1991, 149-164, <https://doi.org/10.1007/BF00026049>, 1990.

568 Kolar, V., Vlašánek, P., and Boukal, D.S.: The influence of successional stage on local odonate communities in
569 man-made standing waters. *Ecol. Eng.*, 173, 106440, <https://doi.org/10.1016/j.ecoleng.2021.106440>, 2021.

570 Kopáček, J. and Hejzlar, J.: Semi-micro determination of total phosphorus in fresh waters with perchloric acid
571 digestion. *Int. J. Environ. Anal. Chem.*, 53, 173-183, <https://doi.org/10.1080/03067319308045987>, 1993.

572 Kopáček, J. and Procházková, L.: Semi-Micro Determination of Ammonia in Water by the Rubazoic Acid Method.
573 *Int. J. Environ. Anal. Chem.*, 53, 243-248, <https://doi.org/10.1080/03067319308045993>, 1993.

574 Kosten, S., Almeida, R.M., Barbosa, I., Mendonça, R., Muzitano, I.S., Oliveira-Junior, E.S., Vroom, R.J.E., Wang,
575 H.J., and Barros, N.: Better assessments of greenhouse gas emissions from global fish ponds needed to adequately
576 evaluate aquaculture footprint. *Sci. Total Environ.*, 748, 141247, <https://doi.org/10.1016/j.scitotenv.2020.141247>,
577 2020.

578 Laas, A., Noges, P., Koiv, T., and Noges, T.: High-frequency metabolism study in a large and shallow temperate
579 lake reveals seasonal switching between net autotrophy and net heterotrophy. *Hydrobiologia*, 694, 57-74,
580 <https://doi.org/10.1007/s10750-012-1131-z>, 2012.

581 Loken, L.C., Crawford, J.T., Schramm, P.J., Stadler, P., Desai, A.R., and Stanley, E.H.: Large spatial and temporal
582 variability of carbon dioxide and methane in a eutrophic lake. *J. Geophys. Res. Biogeosci.*, 124, 2248-2266
583 <https://doi.org/10.1029/2019JG005186>, 2019.

584 Lüdecke, D.: “ggeffects: Tidy Data Frames of Marginal Effects from Regression Models.” *J. Open Source Soft.*,
585 3, 772, <https://doi.org/10.21105/joss.00772>, 2018.

586 Lüdecke, D., Makowski, D., and Waggoner, P.: performance: Assessment of Regression Models Performance. R
587 package version 0.4.4. <https://CRAN.R-project.org/package=performance>, 2020.

588 Ma, Y., Sun, L., Liu, C., Yang, X., Zhou, W., Yang, B., Schwenke, G., and Liu, D.L.: A comparison of methane
589 and nitrous oxide emissions from inland mixed-fish and crab aquaculture ponds. *Sci. Total Environ.*, 637-638,
590 517-523, <https://doi.org/10.1016/j.scitotenv.2018.05.040>, 2018

591 McAuliffe, C.: Gas Chromatographic determination of solutes by multiple phase equilibrium. *Chem. Technol.*, 1,
592 46-51, 1971.

593 Miranda, L.E., Hargreaves, J.A., and Raborn, S.W.: Predicting and managing risk of unsuitable dissolved oxygen
594 in a eutrophic lake. *Hydrobiologia*, 457, 177-185, <https://doi.org/10.1023/A:1012283603339>, 2001.

595 Murphy, J. and Riley, J.P.: A modified single-solution method for the determination of phosphate in natural waters.
596 *Anal. Chim. Acta*, 27, 31-36, [https://doi.org/10.1016/S0003-2670\(00\)88444-5](https://doi.org/10.1016/S0003-2670(00)88444-5), 1962.

597 Natchimuthu, S., Sundgren, I., Gålfalk, M., Klemetsson, L., Crill, P., Danielsson, Å., and Bastviken, D.: Spatio-
598 temporal variability of lake CH₄ fluxes and its influence on annual whole lake emission estimates. *Limnol.*
599 *Oceanogr.*, 61, 13-26, <https://doi.org/10.1002/lno.10222>, 2016.

600 Nijman, T.P.A., Lemmens, M., Lurling, M., Kosten, S., Welte, C., and Veraart, A.J.: Phosphorus control and
601 dredging decrease methane emissions from shallow lakes. *Sci. Total Environ.*, 847, 15758,
602 <https://doi.org/10.1016/j.scitotenv.2022.157584>, 2022.

603 Ortiz, D.A. and Wilkinson, G.M.: Capturing the spatial variability of algal bloom development in a shallow
604 temperate lake. *Freshwater Biol.*, 66, 2064-2075, <https://doi.org/10.1111/fwb.13814>, 2021.

605 ~~Ostrovsky, I., McGinnis, D.F., Lapidus, L., and Eckert, W.: Quantifying gas ebullition with echosounder: The role
606 of methane transport by bubbles in a medium sized lake. *Limnol. Oceanogr. Meth.*, 6, 105-118,
607 <https://doi.org/10.4319/lom.2008.6.105>, 2008.~~

608 Pechar, L.: Impacts of long-term changes in fishery management on the trophic level and water quality in Czech
609 fishponds. *Fisheries Manag. Ecol.*, 7, 23-32, 10.1046/j.1365-2400.2000.00193.x, 2000.

610 Pokorný, J. and Hauser, V.: The restoration of fish ponds in agricultural landscapes. *Ecol. Eng.*, 18, 555-574,
611 [https://doi.org/10.1016/S0925-8574\(02\)00020-4](https://doi.org/10.1016/S0925-8574(02)00020-4), 2002.

612 ~~Podgrajsek, E., Sahlée, E., Bastviken, D., Holst, J., Lindroth, A., Tranvik, L., and Rutgersson, A.: Comparison of
613 floating chamber and eddy covariance measurements of lake greenhouse gas fluxes, *Biogeosciences*, 11, 4225-
614 4233, <https://doi.org/10.5194/bg-11-4225-2014>, 2014.~~

615 Potužák, J., Hůda, J., and Pechar, L.: Changes in fish production effectivity in eutrophic fishponds – impact of
616 zooplankton structure. *Aquacult. Int.*, 15, 201-210, <https://doi.org/10.1007/s10499-007-9085-2>, 2007.

617 Potužák, J., Duras, J., and Drozd, B.: Mass balance of fishponds: are they sources or sinks of phosphorus?
618 *Aquacult. Int.*, 24, 1725-1745, <https://doi.org/10.1007/s10499-016-0071-4>, 2016.

619 Prairie, Y.T. and del Giorgio, P.A.: A new pathway of freshwater methane emissions and the putative importance
620 of microbubbles. *Inland Waters*, 3, 311-320, <https://doi.org/10.5268/IW-3.3.542>, 2013.

621 Procházková, L.: Bestimmung der Nitrate im Wasser. *Zeitschrift für Analytische Chemie*, 167, 254-260, 1959.

622 Rasilo, T., Prairie, Y.T., and del Giorgio, P.A.: Large-scale patterns in summer diffusive CH₄ fluxes across boreal
623 lakes, and contribution to diffusive C emissions. *Glob. Change Biol.*, 21, 1124-1139,
624 <https://doi.org/10.1111/gcb.12741>, 2015.

625 R Core Team: A language and environment for statistical computing. R Foundation for Statistical Computing.
626 Vienna, Austria <https://www.R-project.org/>, 2018.

627 Reynolds, C.S.: *Ecology of phytoplankton*, Cambridge University Press, Cambridge,
628 <https://doi.org/10.1017/CBO9780511542145>, 2006.

629 Rinke, K., Huber, A.M.R., Kempke, S., Eder, M., Wolf, T., Probst, W.N., and Rothhaupt, K.: Lake-wide
630 distributions of temperature, phytoplankton, zooplankton, and fish in the pelagic zone of a large lake. *Limnol.*
631 *Oceanogr.*, 54, 1306-1322, <https://doi.org/10.4319/lo.2009.54.4.1306>, 2009.

632 Rutegwa, M., Potužák, J., Hejzlar, J., and Drozd, B.: Carbon metabolism and nutrient balance in a hypereutrophic
633 semi-intensive fishpond. *Knowl.Manag. Aquat. Ecosyst.*, 49, <https://doi.org/10.1051/kmae/2019043>, 2019.

634 Sanseverino, A.M., Bastviken, D., Sundh, I., Pickova, J., and Enrich-Prast, A.: Methane carbon supports aquatic
635 food webs to the fish level. *PLoS One*7, e42723, <https://doi.org/10.1371/journal.pone.0042723>, 2012.

636 Scheffer, M.: *Ecology of shallow lakes. Population and Community Biology Series*. Springer, 357 p.,
637 <https://doi.org/10.1007/978-1-4020-3154-0>, 2004.

638 Schilder, J., Bastviken, D., van Hardenbroek, M., Kankaala, P., Rinta, P., Stötter, T., and Heiri, O.: Spatial
639 heterogeneity and lake morphology affect diffusive greenhouse gas emission estimates of lakes. *Geophys. Res.*
640 *Lett.*, 40, 5752-5756, <https://doi.org/10.1002/2013GL057669>, 2013.

641 Schmiedeskamp, M., Praetzel, L.S.E., Bastviken, D., and Knorr, K.H.: Whole-lake methane emissions from two
642 temperate shallow lakes with fluctuating water levels: Relevance of spatiotemporal patterns. *Limnol. Oceanogr.*,
643 66, 2455-2469, <https://doi.org/10.1002/lno.11764>, 2021.

644 [Schubert, C.J., Diem, T., Eugster W.: Methane emissions from a small wind shielded lake determined by eddy](#)
645 [covariance, flux chambers, anchored funnels, and boundary model calculations: a comparison. *Environ. Sci.*](#)
646 [*Technol.*, 46, 4515-4522, <https://doi.org/10.1021/es203465x>, 2012](#)

647 Stanley, E.H., Collins, S.M., Lottig, N.R., Oliver, S.K., Webster, K.E., Cheruvilil, K.S., and Soranno, P.A.: Biases
648 in lake water quality sampling and implications for macroscale research. *Limnol. Oceanogr.*, 64, 1572-1585,
649 <https://doi.org/10.1002/lno.11136>, 2019.

650 Stockwell, J.D., Doubek, J.P., Adrian, R., Anneville, O., Carey, C.C., Carvalho, L., Domis, L.N.D.S., Dur, G.,
651 Frassl, M.A., Grossart, H.-P., Ibelings, B.W., Lajeunesse, M.J., Lewandowska, A.M., Llames, M.E., Matsuzaki,
652 S.-I.S., Nodine, E.R., Nöges, P., Patil, V.P., Pomati, F., Rinke, K., Rudstam, L.G., Rusak, J.A., Salmaso, N.,
653 Seltmann, C.T., Straile, D., Thackeray, S.J., Thiery, W., Urrutia-Cordero, P., Venail, P., Verburg, P., Woolway,
654 R.I., Zohary, T., Andersen, M.R., Bhattacharya, R., Hejzlar, J., Janatian, N., Kpodonu, A.T.N.K., Williamson,
655 T.J., and Wilson, H.L.: Storm impacts on phytoplankton community dynamics in lakes. *Glob. Change Biol.*, 26,
656 2756-2784, <https://doi.org/10.1111/gcb.15033>, 2020.

657 ~~Tranvik, L.J., Downing, J.A., Cotner, J.B., Loiselle, S.A., Striegl, R.G., Ballatore, T.J., Dillon, P., Finlay, K.,~~
658 ~~Fortino, K., Knoll, L.B., Kortelainen, P.L., Kutser, T., Larsen, S., Laurion, I., Leece, D.M., McCallister, S.L.,~~
659 ~~McKnight, D.M., Melack, J.M., Overholt, E., Porter, J.A., Prairie, Y.T., Renwick, W.H., Roland, F., Sherman,~~
660 ~~B.S., Schindler, D.W., Sobek, S., Tremblay, A., Vanni, M.J., Verschoor, A.M., von Wachenfeldt, E.,~~

661 ~~Weyhenmeyer, G.A.: Lakes and reservoirs as regulators of carbon cycling and climate. *Limnol. Oceanogr.*, 54,~~
662 ~~2298-2314, https://doi.org/10.4319/lo-2009.54.6-part_2.2298, 2009.~~

663 van Bergen, T.J.H.M., Barros, N., Mendonça, R., Aben, R.C.H., Althuisen, I.H.J., Huszar, V., Lamers, L.P.M.,
664 Lüring, M., Roland, F., Kosten, S.: Seasonal and diel variation in greenhouse gas emissions from an urban pond
665 and its major drivers. *Limnol. Oceanogr.*, 64, 2129-2139, <https://doi.org/10.1002/lno.11173>, 2019.

666 Varadharajan, Ch. and Hemond, H.F.: Time-series analysis of high-resolution ebullition fluxes from a stratified,
667 freshwater lake. *J. Geophys. Res.*, 117, G02004, <https://doi.org/10.1029/2011JG001866>, 2012.

668 Wanninkhof, R.: Relationship between wind speed and gas exchange over the ocean revisited. *Limnol. Oceanogr.*
669 *Methods*, 12, 351-362, <https://doi.org/10.4319/lom.2014.12.351>, 2014.

670 Wiesenburg, D.A. and Guinasso N.L.: Equilibrium solubilities of methane, carbon monoxide, and hydrogen in
671 water and sea water. *J. Chem. Eng. Data*, 24, 356-360, <https://doi.org/10.1021/je60083a006>, 1979.

672 Wik, M., Varner, R.K., Anthony, K.W., MacIntyre, S., and Bastviken, D.: Climate-sensitive northern lakes and
673 ponds are critical components of methane release. *Nat. Geosci.*, 9, 99-105, <https://doi.org/10.1038/ngeo2578>,
674 2016.

675 Xiao, Q., Zhang, M., Hu, Z., Gao, Y., Hu, Ch., Liu, Ch., Liu, S., Zhang, Z., Zhao, J., Xiao, W., and Lee, X.: Spatial
676 variations of methane emission in a large shallow eutrophic lake in subtropical climate. *J. Geophys. Res.*
677 *Biogeosci.*, 122, <https://doi.org/10.1002/2017JG003805>, 2017.

678 Yamamoto, S., Alcauskas, J.B., and Crozier, T.E. Solubility of methane in distilled water and seawater. *J. Chem.*
679 *Eng. Data*, 21, 78-80, <https://doi.org/10.1021/je60068a029>, 1976.

680 Yan, X., Xu, X., Ji, M., Zhang, Z., Wang, M., Wu, S., Wang, G., Zhang, Ch., and Liu, H.: Cyanobacteria blooms:
681 A neglected facilitator of CH₄ production in eutrophic lakes. *Sci. Total Environ.*, 651, 466-474,
682 <https://doi.org/10.1016/j.scitotenv.2018.09.197>, 2019.

683 Yang, P., Zhang, Y., Yang, H., Zhang, Y., Xu, J., Tan, L., Tong, C., and Lai, D.Y.: Large fine-scale spatiotemporal
684 variations of CH₄ diffusive fluxes from shrimp aquaculture ponds affected by organic matter supply and aeration
685 in Southeast China. *J. Geophys. Res. Biogeosci.*, 124, 1290-1307, <https://doi.org/10.1029/2019JG005025>, 2019.

686 Yang, P., Zhang, Y., Yang, H., Guo, Q., Lai, D.Y.F., Zhao, G., Li, L., and Tong, C.: Ebullition was a major
687 pathway of methane emissions from the aquaculture ponds in Southeast China. *Water Res.*, 184, 116176,
688 <https://doi.org/10.1016/j.watres.2020.116176>, 2020.

689 Yuan, J., Xiang, J., Liu, D.Y., Kang, H., He, T.H., Kim, S., Lin, Y.X., Freeman, C., and Ding, W.X.: Rapid growth
690 in greenhouse gas emissions from the adoption of industrial-scale aquaculture. *Nat. Clim. Chang.*, 9, 318-322,
691 <https://doi.org/10.1038/s41558-019-0425-9>, 2019.

692 Yuan, J., Liu, D., Xiang, J., He, T., Kang, H., and Ding, W.: Methane and nitrous oxide have separated production
693 zones and distinct emission pathways in freshwater aquaculture ponds. *Water Research*, 190, 116739,
694 <https://doi.org/10.1016/j.watres.2020.116739>, 2021.

695 Zar, J.H.: *Biostatistical analysis*. Prentice Hall, Inc., Englewood Cliffs, New York, 663 p., 1984.

696 Zhang, L., Liao, Q., Gao, R., Luo, R., Liu, Ch., Zhong, J., and Wang, Z.: Spatial variations in diffusive methane
697 fluxes and the role of eutrophication in a subtropical shallow lake. *Sci. Total Environ.*, 759, 143495,
698 <https://doi.org/10.1016/j.scitotenv.2020.143495>, 2021.

699 Zhao, J., Zhang, M., Xiao, W., Jia, L., Zhang, X., Wang, J., Zhang, Z., Xie, Y., Yini Pu, Liu, S., Feng, Z., Lee X.:
700 Large methane emission from freshwater aquaculture ponds revealed by long-term eddy covariance observation.
701 *Agric. For. Meteorol.*, 308-309, 108600, <https://doi.org/10.1016/j.agrformet.2021.108600>, 2021.
702 Zhou, Y.Q., Zhou, L., Zhang, Y.L., de Souza, J.G., Podgorski, D.C., Spencer, R.G.M., Jeppesen, E., and Davidson,
703 T.A.: Autochthonous dissolved organic matter potentially fuels methane ebullition from experimental lakes. *Water*
704 *Res.*, 166, 115048, <https://doi.org/10.1016/j.watres.2019.115048>, 2019.
705 Zuur, A.F., Ieno, E.N., Walker, N.J., Saveliev, A.A., and Smith, G.M.: *Mixed effects models and extensions in*
706 *ecology with R*. Springer, New York, USA, 574 p, <https://doi.org/10.1007/978-0-387-87458-6>, 2009.
707

